ROYAL SOCIETY OF CHEMISTRY

PERSPECTIVE

Check for updates

S 2B or not 2B?

Ian Dance (ORCID)

In recent years a large collection of experimental information has prompted proposals that an atom, S2B, part of the catalytic metal cluster FeMo-co of the enzyme nitrogenase, is displaced during the enzyme mechanism in order to allow the binding of substrate N_2 to the adjacent Fe atoms. Computational investigation has generated a complete enzyme mechanism in which S2B is retained in its resting state position, and as such is an *essential* agent in the enzyme mechanism. A dilemma arises, between a disruptive mechanism – with S2B moved out of the way during the reaction steps – and a conservative mechanism – with S2B retained and necessarily used. Following the Prince of Denmark, is the 2B position of FeMo-co to be S or not to be S? I have assembled the evidence and arguments in this Perspective.

1 Introduction

Conversion of inert N_2 to NH_3 is a chemically difficult transformation. It is remarkable that the bacterial enzyme nitrogenase effects this transformation under mild ambient conditions, supporting about half of the world's food supply.[1,2] How does the enzyme fix nitrogen so easily? Despite many decades of research the chemical mechanism of nitrogenase is uncertain.[3,4] The enzyme stoichiometry is $N_2 + 8e^- + 8H^+ \rightarrow 2NH_3 + H_2$. Nitrogenase comprises two proteins, component 1

School of Chemistry, UNSW Sydney, NSW 2052, Australia.
E-mail: i.dance@unsw.edu.au

Ian Dance started research in Sydney with metalloprotein crystallographer Hans Freeman. Since then his research has spanned the fields of chemical crystallography, exploratory inorganic synthesis, metal chalcogenide cluster compounds, metal thiolate compounds, metallocarbohedrenes, mass spectrometry and gas phase inorganic chemistry, crystal packing and supramolecular chemistry, and intermolecular motifs and their energies. Following revelation of the structure of the nitrogenase protein in 1992 he was inspired to return to an early interest in metalloenzymes, and has published 45 papers on the chemistry of secretive nitrogenase.
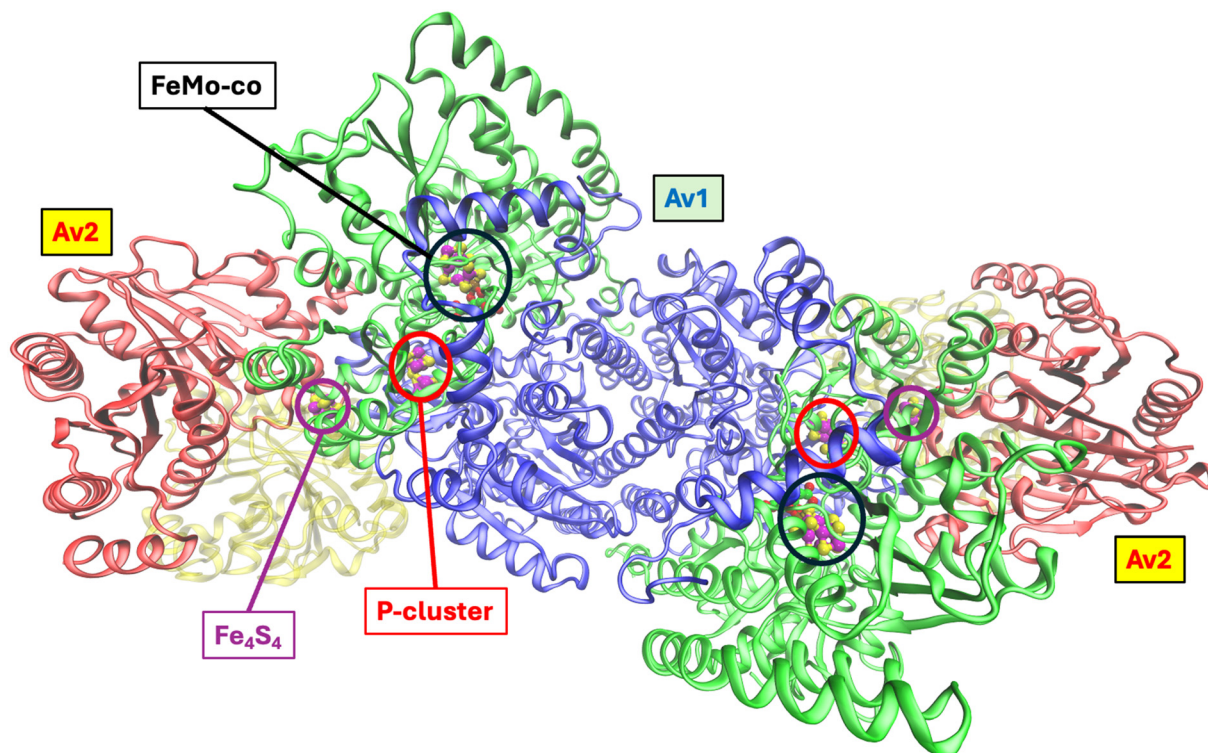
Ian Dance

which contains the active site cofactor FeMo-co and another iron cluster (the P cluster) controlling electron supply, together with component 2, a reductase Fe protein containing an Fe_4S_4 cluster and the ATP hydrolysis machinery. The structure of the *Azotobacter vinelandii* (*Av*) enzyme with the reductase protein (*Av*2) bound to *Av*1 is shown in Fig. 1, which also shows the locations of FeMo-co, the P-cluster, and the Fe_4S_4 cluster at the interface of the two components. The biochemical mechanism involves repeated (8 times) association and dissociation of reductase component 2 protein and catalytic component 1 protein, each resulting in the transfer of an electron to FeMo-co, *via* the P-cluster, from the Fe_4S_4 cluster. There are three isozymes, with metals Mo, V or Fe as part of the catalytic cofactor, named FeMo-co, FeV-co and FeFe-co.[3] The isozyme component 1 proteins are named MoFe, VFe and FeFe. Mo nitrogenase is the most efficient in reducing N_2, while V nitrogenase is able to reduce CO (which is a strong non-competitive inhibitor of Mo nitrogenase).

Fig. 2 shows the structure of FeMo-co, an Fe_7MoCS_9 cluster with the tricarboxylic acid homocitrate as bidentate ligand to Mo. His442 provides the sixth ligand for Mo and cysteine 275 completes tetrahedral coordination of Fe1. Three surrounding residues form hydrogen bonds (black-white striped) with FeMo-co, and of these the most consequential is the hydrogen bond from Nε–H of His195 to atom S2B which bridges Fe2 and Fe6. S2B and the other two doubly-bridging atoms S5A and S3A are termed 'belt' S atoms. Mutagen-reactivity experiments show that the active domain of FeMo-co is the front face, Fe2–S2B–Fe6–S3B–Fe7 enclosed by Val70 and Arg96.[6–13,14–16]

Intermediates in the catalytic conversion are commonly labelled E1, E2···to E8, as originally devised by Thorneley and Lowe[17] and indicating the number of added electrons (*i.e.* the number of component 2-component 1 associations). There is a fundamental experimental impediment to the isolation and

Fig. 1 The structure (PDB 1N2C) of the *Av*1 protein of Mo nitrogenase, bound with two *Av*2 proteins.[5] *Av*1 is a dimer of two α (green) β (blue) sub-units. Locations of FeMo-co, the P-cluster, and the Fe_4S_4 cluster at the *Av*2–*Av*1 interface, are marked.
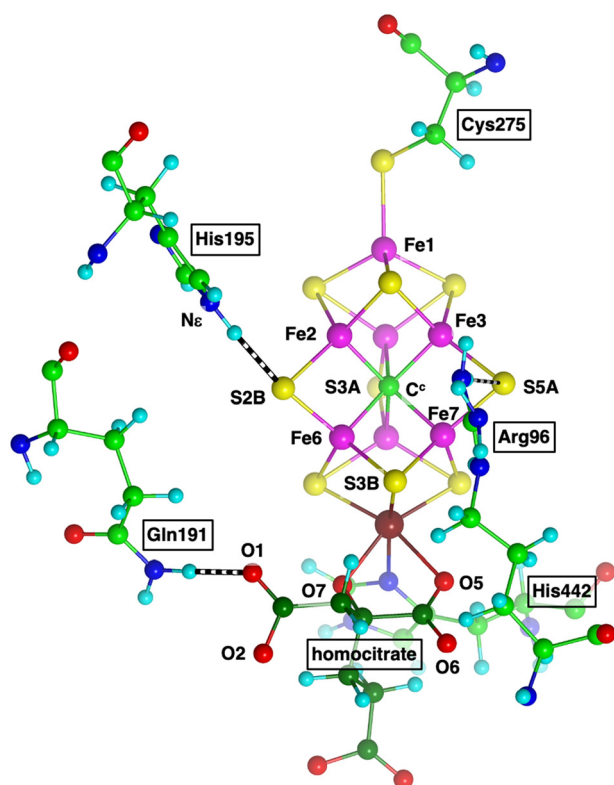

Fig. 2 The structure of FeMo-co, with key surrounding residues that comprise the active site. Hydrogen bonds are striped. In FeV-co a bridging CO_3 ligand replaces S3A at the rear.

direct investigation of intermediates because unavoidable protons are a substrate of the enzyme, and mixtures of transient intermediates occur.[3,18] Furthermore, the overall chemical reaction implies a mechanistic cycle with at least 27 steps: eight introductions of a proton, eight additions of an electron, N_2 binding, breaking the N–N bond, formation of six N–H bonds, two dissociations of NH_3 and formation of one H–H bond.

After the first crystal structure (1992) of the MoFe protein and first view of the cofactor,[19] the unusual C-centering of FeMo-co was revealed through an auspicious protein crystal structure in 2011.[20] This is the resting state of the enzyme. However, after just three years, additional crystal structures with altered forms of the cofactor were reported, and stimulated questions about the structure of the cofactor during enzyme turnover, and the chemical mechanism.

2 Experiments yielding altered forms of FeMo-co and FeV-co

2.1 S2B in FeMo-co replaced by CO

In 2014 it was reported that a crystal of MoFe protein from species *Azotobacter vinelandii* (*Av*) obtained under turnover conditions (*i.e.* in the presence of ATP and with dithionite providing reducing equivalents) but in the presence of the non-competitive inhibitor CO, contained a modified structure of

the cofactor. Bridging CO replaced S2B as the bridge between Fe2 and Fe6.[21] Additional electron density was evident 22 Å away from FeMo-co, and was suggested as a possible location for displaced S2B. The authors speculated that the binding of substrate N_2 at the S2B site could be enhanced by reversible dissociation of S2B.

This was the genesis of a concept of labile S2B as part of the physiological catalysis. The argument was strengthened by additional observations that crystals of this CO-inhibited MoFe-protein, when dissolved in an assay mixture in the absence of CO, were active for reduction of the alternative substrate C_2H_2. Subsequent crystallisation of the reactivated protein showed that it returned to the resting state form of FeMo-co with S2B in place.[21]

2.2 Belt S in FeMo-co substituted by Se

One year later the Rees group reported explorations of selenocyanate $SeCN^-$ as an alternative substrate, finding it to be a potent yet reversible inhibitor of C_2H_2 reduction. Incubation of Mo nitrogenase under turnover conditions with $SeCN^-$ sufficient to inhibit C_2H_2 reduction, yielded crystals in which S2B of FeMo-co was replaced by Se.[22] This Se substituted protein, named Av1-Se2B, retained acetylene and dinitrogen reduction activity. Surprisingly, while Se2B substituted FeMo-co was turning over with acetylene reduction, the Se atom migrated to the other two belt positions, 3A and 5A. Some migration was detected after just a few acetylene reduction cycles, but thereafter the rate of migration was slow relative to the number of reduction cycles. The location of displaced S was not determined. After several thousand turnovers with acetylene as substrate and dithionite as reductant all Se was lost and S returned to the 2B position. Exposure of the Av1-Se2B protein to CO under turnover conditions led to replacement of Se2B by CO and, remarkably, migration of Se to the other 3A and 5A belt positions. In total, these experiments revealed a lability of not only S2B, but also S3A and S5A. The authors speculated that the belt S atoms might be shielding coordination positions of the cofactor Fe atoms, and that S displacement could activate the cofactor for substrate binding. Theoretical investigation of these reactions, which require C_2H_2 or CO for migration of the belt groups, reached the conclusion that these reactions could be accounted for with standard non-enzymatic reactions involving the small molecules SCO, SeCO, C_2H_2S, C_2H_2Se, $SeCN^-$, SCN^- functioning as carriers of S and Se atoms.[23]

2.3 S2B in FeV-co replaced by a light atom

Vanadium nitrogenase differs from the Mo isozyme in being able to reduce CO to ethylene and other hydrocarbons, and in possessing a modified cofactor FeV-co that contains a bridging carbonate ligand replacing the bridging sulfur atom, S3A.[24] In 2018 the Einsle group discovered that if V nitrogenase was isolated in the presence of restricted supply of dithionite as reductant, crystallisation yielded a structure in which S2B had been replaced by a smaller atom, proposed to be NH,[25] but probably OH.[26,27] In this crystal structure (PDB 6FEA) new electron density appeared in a

protein cavity 7 Å from the resting S2B position, and was proposed to be displaced SH^- in a holding site, hydrogen bonded to backbone amides of two surrounding residues. This putative reaction intermediate is illustrated in Fig. 3.

2.4 S2B in FeV-co replaced by CO

In 2020 it was reported that V nitrogenase, crystallised after turnover in the presence of CO alone, showed a structure with CO bridging Fe2 and Fe6 (PDB 7ADR).[28] There was no evidence of the S or SH displaced from the S2B position. This Fe2–CO–Fe6 bridged structure was found to be remarkably stable. After further turnover with CO replaced by Ar, crystallisation revealed a cofactor with mainly OH but small proportion of S in the bridging position (PDB 7ADR). In addition, electron density attributed to S appeared in the SH^- 'holding site'. This returning S that appeared (crystal 7ADR) after CO removal was suggested to be sourced from excess dithionite in the turnover system. The authors noted that SH^- and Cl^- would be indistinguishable in the SH^- 'holding site'.

Also, crystal structures are reported for both the Mo (PDB 7JRF)[29] and V (PDB 7AIZ)[30] cofactors with two bound CO molecules, one bridging Fe2 and Fe6, the other as terminal Fe6–CO at the *exo* position of Fe6.

2.5 Belt S in FeMo-co replaced by N_2

On the premise that when the reductant, dithionite, that drives the turning-over enzyme is depleted, the catalytic cycle
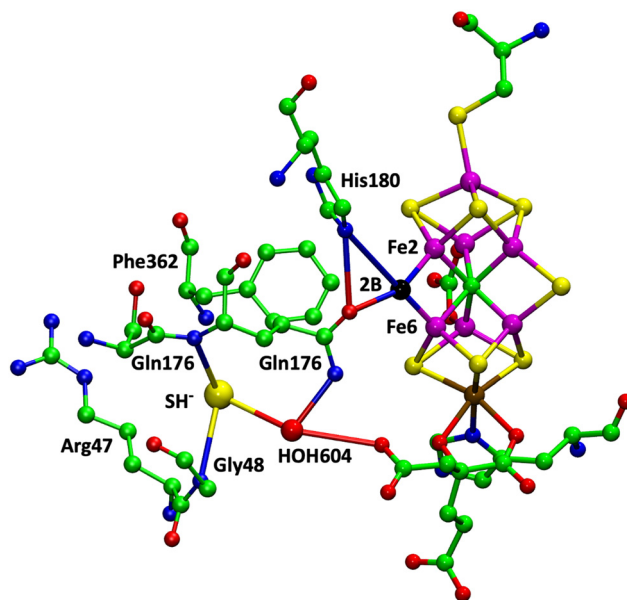

Fig. 3 Key features of the VFe protein structure reported by Sippel et al.,[25] PDB 6FEA, α subunit. The uncertain atom at the 2B position is coloured black. The triangular set of bonds between 2B, His180Nε and the reoriented sidechain of Gln176 identify distances in the hydrogen bonding range. Displaced SH^- receives hydrogen bonds from mainchain NH of Gln176 and Gly48, and is hydrogen bonded to HOH604, which also hydrogen bonds to homocitrate carboxylate and the sidechain of Gln176. The remote side of the SH^- pocket is lined with CH functions from Arg47 and Phe362.

will be suspended and trapped in an intermediate stage, the Ribbe group prepared under dithionite-free conditions, an $Av1$ Mo protein, denoted $Av1*$, that was fully functional for N_2 reduction and C_2H_2 reduction when recombined with $Av2$, ATP and dithionite. Crystallisation (within 12 h) and diffraction analysis of $Av1*$ (PDB 6UG0, resolution 1.83 Å) showed two different cofactors, one with altered electron density at the S2B position and the other with altered density at the other two belt positions.[31] These altered densities were modelled as bridge-bound N_2 molecules. Electron density interpreted as the displaced belt S atoms was found at two locations distant 19, 25 Å from their original positions. When $Av1*$ was incubated with $Av2$, ATP and excess dithionite, the $Av1$ protein returned to its resting state structure with all belt S atoms as intact bridges (PDB 6VXT). The validity of these results was challenged by Peters *et al.* on the basis of a re-refinement of the diffraction data, and the biochemical sample preparation.[32] This challenge was rebutted,[33] More significantly, a detailed critical analysis of the diffraction data and its interpretation was published by Ryde *et al.*[34] This revealed that the raw diffraction data was poor and anisotropic, causing the bridging ligands to appear to be diatomic. Incisive quantum refinement of the diffraction data showed that S in the bridging positions gave better results than N_2 or N_2H_2, and led to the conclusion that this structure is better interpreted as resting state FeMo-co.

Further biochemical experiments by Ribbe *et al.* uncovered information about the roles of non-physiological sulfur species in these reactions. The majority of experimental investigations of the nitrogenase reaction use dithionite ($S_2O_4^{2-}$) as the primary reductant, generating sulphite (SO_3^{2-}) as its oxidation product. It was found that $Av1*$ releases product NH_3 only when SO_3^{2-} is supplied together with a different non-physiological sulfur-free reductant, and that in these systems SO_3^{2-} can be converted to S^{2-} which allows recovery of the cofactor after product release.[35,36] These experiments exploring mobilisation of belt S and the possibility that nitrogenase is an atypical sulfite reductase have been extended to V-nitrogenase.[37] Such *in vitro* experiments reveal much about the reactivity of the nitrogenase cofactor, and of dithionite derivatives, but the relevance of this information to the purely physiological mechanism is still to be established.

2.6 S2B in FeFe-co replaced by a light atom

A recent crystal structure of the FeFe protein of Fe-nitrogenase, presumably crystallised after turnover, showed a mixture of two forms (PDB 8BOQ).[38] One form has S2B intact, while the other is proposed to be a turnover state with an unidentified light atom bridging Fe2 and Fe6, and HS^- in a hydrogen bonded holding pocket analogous to that shown in Fig. 3.

2.7 Caveat

The structural information reviewed in the preceding brief history all derives from diffraction analysis of crystals. There is uncertainty about their validity, because (1) the conditions for crystal growth may differ from those of physiological turnover,

(2) crystal growth occurs on a time scale much longer than enzyme turnover, and (3) a single crystal may not report mixed components of the mother liquor. However, the rapidly developing technique of cryo electron microscopy (cryoEM) can diminish these uncertainties.[39–42]

2.8 CryoEM findings

Noting that crystallographic structural studies are limited by their requirements for highly pure, concentrated, isomorphous protein states which hinder the capture of low abundance intermediates, Warmack and Rees deployed cryo electron microscopy[43] to investigate the structural states of nitrogenase that exist at different times in the presence of acetylene, using a pH of 9.5 to decrease the rate of substrate reduction.[44] Turnover was monitored by plunge freezing at 20 s, 5 min, 20 min and 60 min. These samples retain 91%, 62%, 44% and 17% of ethylene production activity, and it was estimated that the first time point captured the initial turnover event. The time-resolved turnover structures of these samples were resolved at nominal resolutions between 1.9 and 2.2 Å. The MoFe protein contains two $\alpha\beta$ dimers (Fig. 1), and one was found to be more disordered in the α subunit at the earlier time points. In the more ordered domain a sequence of structural changes was observed. First there was some depletion of electron density at the S2B position, then depletion of electron density associated with homocitrate, then, approaching 5 min, the cofactor began to distort (mainly at Fe7) and then to be displaced within the surrounding protein. There was no extraneous density observed that might indicate the presence of a displaced sulfur atom. The authors concluded that their time-resolved structures provide experimental support for the displacement of S2B and distortions of the FeMo-cofactor during the first three stages of the substrate reduction mechanism, prior to nitrogen binding.

2.9 Is dithionite a culprit?

All of the experiments described above, except some of those in section 2.5, contained dithionite as non-physiological reductant. As outlined in section 2.5, Ribbe *et al.* have shown that sulfite, generated as the oxidation product of dithionite, can be inserted as sulfide into the cofactor. It is also worth remembering that sulfite reacts with sulfide to form thiosulfate, and that sulfite in turnover mixtures could attack belt sulfide in this way.

Therefore there is some suspicion about the influence of dithionite in crystallisation systems that generated crystals containing FeMo-co with S2B displaced or missing. The use of sulfur-free reductants in these experiments should be informative.

3 Other relevant experimental information

3.1 ENDOR data interpreted

Hoffman and coworkers interpreted ENDOR spectra of freeze-quenched 70^{Ile} protein[45,46] in terms of an E4H4 intermediate

with two belt SH bridges (Fe2–S2BH–Fe6 and Fe3–S5AH–Fe7) coupled with two H bridges (Fe2–H–Fe6) and (Fe3–H–Fe7): there have been some reservations about the data analysis.[47,48] This structure, with retained S2BH bridge, was supported by density functional calculations.[49]

3.2 Observed SH vibrations

Spectroelectrochemical experiments on Mo-nitrogenase turning over under CO and N_2 revealed SH stretching frequencies assigned to terminal SH and doubly bridging SH. The doubly bridging frequencies agreed with calculations for S2B–H as the most stable position for H on S. The authors concluded that the bridge is not lost during turnover.[50]

4   Speculation on the mechanistic role of S2B displacement

The theme of the reports described in section 2 is that S2B is labile and that the cofactor structure can be disrupted. These experimental structural data provoked much speculation that displacement of S2B would generate open coordination positions at *endo*-Fe2 and *endo*-Fe6, and that this would facilitate the binding and activation of N_2.[21,25,28,31,38,44,51,52] Some authors suggested that S2B was a blocking agent, which needed to be displaced so that Fe2 and Fe6 could perform their catalytic role.[22,53,54] Formation of an Fe2–H–Fe6 bridge, proposed to be present in early intermediates, was suggested to require S2B to move away.[25] A vacant S2B site together with an *exo*-Fe6 site are the foundation of the mechanistic concept proposed by Einsle.[52] Ribbe *et al.* introduced a mechanistic concept in which FeMo-co undergoes *ca.* 120° rotations about its pseudo-threefold axis, moving N_2 bound in place of belt S atoms to be close to external protonation sites.[31] This is a "Ferris wheel" mechanism. Norskov and coworkers suggested "a more appropriate label for the unique behaviour of the μ_2-S2B comes not from Janus, but his lover Cardea, the Roman goddess of the hinge. The predicted reversible, hinge-like behaviour of S2B provides a viable mechanism for how this reaction proceeds in nature".[55] Some of these proposed mechanisms assume the existence of serial proton donors adjacent to the intermediates bound at Fe2 and Fe6, but this is not justifiable.[56]

A presumption underlies these suggested mechanisms using displaced S2B to allow substrate binding. This presumption is that both S2B and N_2 (or N_2H_x or NH_y) cannot simultaneously occupy the space between Fe2 and Fe6. It was explicitly claimed that FeMo-co is too crowded if both the substrate and S2B bridge Fe2 and Fe6.[57] However, this view was contradicted by Cao and Ryde[58] who reported a relatively stable calculated structure in which HNNH quadruply bridges an Fe_4 face of FeMo-co, with retention of the contiguous belt sulfide bridges, shown in Fig. 4. The Fe3–Fe7 edge and the Fe4–Fe5 edge are both doubly bridged, by an HN moiety and S5A, S3A respectively. This entity faces the sidechain of Arg359 (not shown).
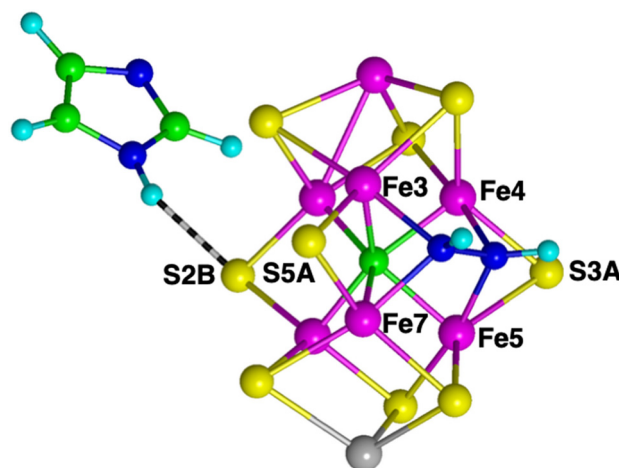

Fig. 4 The Fe3–Fe7–Fe4–Fe5 face of FeMo-co supporting a quadruple HNNH bridge and adjacent belt sulfides, as reported by Cao and Ryde.[58] The calculated Fe–Fe distances are unusually short, 2.46, 2.44, 2.50, 2.48 Å.

I reported calculations demonstrating that, with S2B present and intact, N_2, H or H_2 could bond to Fe2 or to Fe6 in the space between Fe2 and Fe6.[59,60] These ligands occupy the *endo* coordination positions of Fe2 and Fe6, and induce some plasticity of FeMo-co without disruption of the S2B bridge. Structures that are stable both thermodynamically and kinetically were identified.

These computations, together with many results described in section 6 below, show clearly that both S2B and reaction intermediates can simultaneously bridge Fe2 and Fe6, and that the initial presumption is invalid.

5   Computational investigations

The experiments outlined above stimulated numerous computational studies, encompassing (1) the feasibility of reversible unhooking and displacement of S2B or S2BH,[61–63] (2) possible structures of intermediates, and mechanisms, with S2B not bridging Fe2···Fe6,[47,55,57,63–68] and (3) possible structures of intermediates, and mechanisms, with retention of the Fe2–S2B–Fe6 bridge.[47,57,66,67] In the following I survey results that are relevant to the question of the position of S2B through sequences of intermediates in the mechanism.

Prior to the first of the 'labile S2B' experiments, in 2007 Kastner and Blochl reported many calculated structures for N_2 bound to FeMo-co, with S2BH unhooked from Fe6.[69] From these they developed a complete mechanism cycle. In this mechanism (presented pictorially in ref. 70), S2BH remains unhooked throughout, until recovery of the resting state. These calculations were made before identity of the atom at the centre of FeMo-co was confirmed as C, and used N as the central atom. Subsequently these calculations were repeated with C as the central atom and S2BH unhooked from Fe6, with the conclusion that Fe–N–N–Fe bridging, and η^1-N_2

coordination at *endo*-Fe were energetically uncompetitive with η^1-N$_2$ bound at *exo*-Fe6.[71]

Soon after the appearance of S2B deficient crystal structures, Norskov and coworkers presented a density functional computed sequence of intermediates involving first dissociation of S3A as H$_2$S, then formation and dissociation of H$_2$, then binding of N$_2$ and its conversion to N$_2$H, then formation and release of the first NH$_3$, reassociation of H$_2$S, and finally formation and release of the second NH$_3$.[55] Free energies of the intermediates were calculated, but not reaction barriers.

Raugei *et al.* calculated the sequence of intermediates shown in Fig. 5. The N$_2$ binding starts as a μ_2–η^1-N$_2$ bridge with S2BH unhooked, then changes to η^1-N$_2$ at *exo*-Fe2 with rehooked S2BH, then changes back to μ_2–η^1-N$_2$H before bridging as η^2-N$_2$H$_2$ with S2BH unhooked.[49] Relative energies of these intermediates were calculated, together with the reaction barrier for dissociation of H$_2$ from **E4(2H–H2–N2)**.

Bjornsson and coworkers investigated the E4H4 state, and N$_2$ binding to it with evolution of H$_2$, using QM/MM calculations with a 136 atom QM domain.[47] The six most stable optimised models for E4H4 all have unhooked S2BH, with other H atoms variously positioned as Fe-bound H$_2$, or a Fe2–(H)$_2$–Fe6 double bridge, or a single Fe2–H–Fe6 bridge plus *exo*-Fe–H. Calculations of N$_2$ binding to these models considered only end-on bonding at the *exo* positions of Fe2 or Fe6: no structures with N$_2$ bridging Fe2 and Fe6 were reported.

Cao and Ryde[72] investigated computational methods for the E4H4 intermediate, and concluded that the most stable model was consistent with the ENDOR-derived proposal of Hoffman *et al.*,[73] with S2B and S5A both hydrogenated, and with Fe2–H–Fe6 and Fe3–H–Fe7 bridges. The calculated structures have too-short non-bonded contacts (1.47–1.50 Å) between H of Fe3–H–Fe7 and guanidinium H of the Arg96 sidechain, and some suspiciously short (*ca.* 2.44 Å) Fe–Fe distances. These authors then considered possibilities for N$_2$H$_2$ bound to the E0 state of FeMo-co. These are mainly η^1 bonding of HNNH at *exo* positions of Fe, but the quadruply-bridged structure shown in Fig. 4 is distinctive. The corresponding quadruple bridge on the more relevant Fe2–Fe6–Fe3–Fe7 face was also described: in this the guanidinium H of Arg96 transferred to S5A.[58]

Jiang and Ryde explored N$_2$ binding to the E0–E4 states, but considered only end-on coordination of N$_2$ at the *exo* positions

of Fe2 or Fe6. No stable structures with bound N$_2$ and an intact Fe2–S2BH–Fe6 bridge were found.[67] These authors also calculated a sequence of intermediates, starting from E4 with HNNH η^1 bound at *exo*-Fe6, proceeding through HNNH$_2$, then H$_2$NNH$_2$ at the same position, then release of the first NH$_3$, and finally formation of the second NH$_3$ at *exo*-Fe6 and dissociation.[57] These intermediates retain the Fe2–S2B–Fe6 bridge, but, strangely, it was calculated as S2B, not the stable S2BH form. A following publication reported calculations with S2B hydrogenated, because the authors intended to facilitate unhooking of S2BH.[74] This investigation developed a sequence of the most stable intermediates from the E4 N$_2$H$_2$ state through E5, E6, E7 and E8, returning to E0. The E4, E5 and E6 structures contain bridged S2BH with HNNH, HNNH$_2$ and H$_2$NNH$_2$ respectively coordinated at *exo*-Fe2. Then followed three successive E7 intermediates shown in Fig. 6. Significant results are: (1) the bond from Fe6 to NH$_2$NH$_3$ is very long (2.57 Å); (2) despite the expectation of S2BH unhooking, S2BH was retained in all except one intermediate (**E7–NH$_2$ + NH$_3$**) where it was substituted by Fe2–NH$_2$–Fe6; (3) the His195NϵH⋯S2B hydrogen bond is ineffective in **E7–NH$_2$ + NH$_3$**; (4) the homocitrate proton was used to convert bridging NH$_2$ to Fe6–NH$_3$; (5) Fe–S2B distances are elongated from *ca.* 2.3 to *ca.* 2.7 Å when that Fe is coordinated at its *exo* position. It is difficult to envisage a reaction pathway from **E7–H$_2$NNH$_3$** to **E7–NH$_2$ + NH$_3$**, requiring distal NH$_3$ on the *exo* Fe6–H$_2$NNH$_3$ intermediate to move a long way to the *exo* position of Fe2.

Jiang and Ryde concluded that "half-dissociation of S2B needs to be considered in the reaction mechanism of nitrogenase but seems to be of minor importance during the second half-reaction".[74]

A crucial aspect of mechanism is the introduction of protons and migration of H atoms on FeMo-co, in preparation for transfer to N in the sequence of intermediates. Ryde and coworkers reported a detailed investigation of proton transfers within the FeMo cluster, assuming that the proton enters on either S3B, S4B or S5A, and is then transported to the substrate *via* the sulfide and Fe atoms.[66] They found that the net barriers for the proton transfers are in general larger (107–213 kJ mol^{-1}) when S2B has fully dissociated from the cluster than if S2B remains bound (69–83 kJ mol^{-1}). They concluded that their results provide a strong argument against the dissociation of S2B.
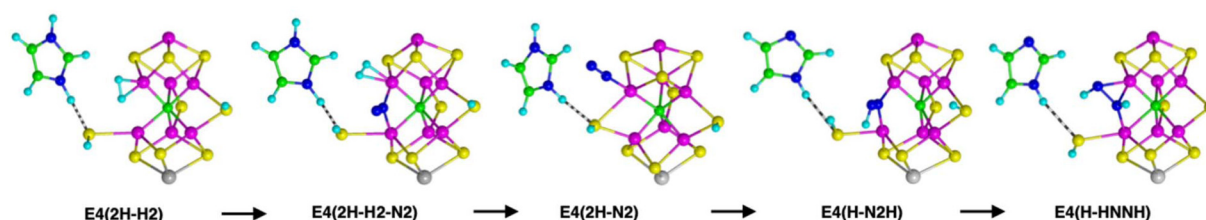

Fig. 5 The sequence of intermediates calculated by Raugei *et al.*, with original labels, redrawn with coordinates provided.[49] Note the unusual orientation of His195 sidechain and the change in its protonation in the last two structures.
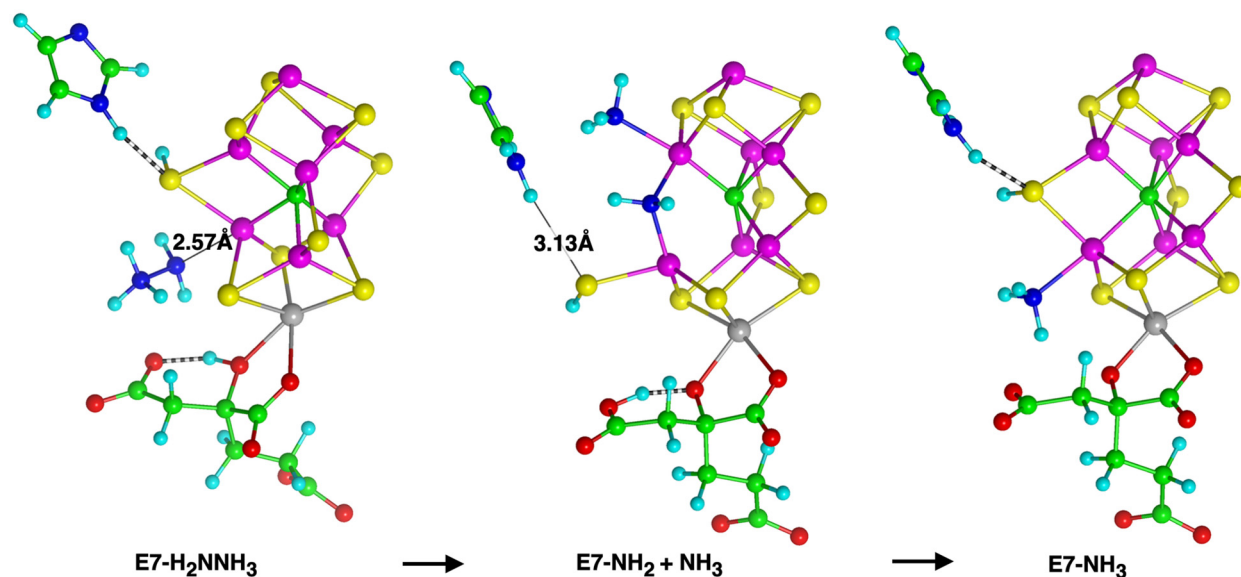
Fig. 6 Three successive E7 intermediates in the sequence described in ref. 74, redrawn from coordinates provided.

Siegbahn's calculations on sulfide release were based on an unusual model containing H bound in the Fe1, Fe2, Fe4 part of FeMo-co. One report[65] described dissociation of belt S3A as H_2S, while another concluded that non-belt S1A could dissociate as H_2S, and that S2B would not dissociate.[75] These calculations are not related to the experimental structures.

Cao and Ryde[64] undertook QM/MM calculations on an S2B deficient model based on the crystal structure of V-nitrogenase in a putative turnover state, section 2.3 above. The 170–178 atom QM model (using Mo) contained the side chain of Gln191 flipped towards the vacant S2B position (see Fig. 3) but did not contain displaced SH^-. The sequence of calculated intermediates, shown in Fig. 7, started at the first binding of N_2 (**E4-NN**) and continued to formation of the second NH_3 (**E8-NH₃**) before reversion to E0 with re-configuration of the Gln191 sidechain and regeneration of S2B.

I have developed a complete mechanism for the nitrogenase catalytic cycle in which the Fe2–S2B–Fe6 bridge is retained and N_2 is bound, activated, and fully reduced in a reaction domain between Fe2 and Fe6. The intact S2B bridge is a significant and *necessary* component of this mechanism, as described in the next section.

6 The complete conservative mechanism with retained S2B

The mechanism outlined here is based on and supported by validated density functional calculations using a 483+ atom model including all relevant protein surrounds. Full details of the computational model, procedures, and the results used in developing this mechanism are provided in five recent papers.[76–80] Throughout the following description the number of electrons and protons added at each stage is

shown in the status boxes. All protons are introduced sequentially from the external medium by Grotthuss translocation along the proton wire, and transferred to S3B.[81] Ryde and co-workers have pointed out that an incoming proton is more stably located on the alternative nearby sulfur atoms S5A and S4B than on S3B.[66] A proton at S5A or S4B is less mechanistically competent than it is at S3B. They also calculated that, if the S2B bridge is intact, a proton on S5A can migrate to S3B *via* Fe7. Further, they tested the hypothesis that S5A is protonated and non-functional throughout the mechanism, and found that this decreased reaction barriers in their mechanism. I calculate that electron addition to FeMo-co increases the basicity of its S atoms, and that electronation of FeMo-co could be the trigger for proton transfer from the proton wire.[80] Electron and proton addition creates an H atom on S3B, from which it can migrate to other atoms of FeMo-co.[82] This $e^- + H^+ = H$ introduction and migration occurs eight times during the mechanism, and is symbolised as arrow clusters in the reaction schemes. Reaction energies and kinetic barriers mentioned in the following are ranges, for different electronic states of the systems, as detailed in the papers cited.

The first section of the mechanism[76,78] is outlined in Scheme 1, which also defines labels for intermediates, and provides commentary on the reaction steps. It is necessary to explain at the outset the occurrence of N_2 bound end-on at the *exo* position of Fe2 in some intermediates. In the protein there is a well defined channel for ingress of N_2 from the exterior.[83–86] This channel leads directly to the *exo* coordination position of Fe2, where N_2 can bind end-on with variable thermodynamics.[79] However there are no surrounding H donors, and this *exo*-Fe2–N_2 cannot be reduced. It is 'non-reducible N_2', and has a role to block the *exo*-Fe2 position and keep intermediates in the *endo* space between Fe2 and
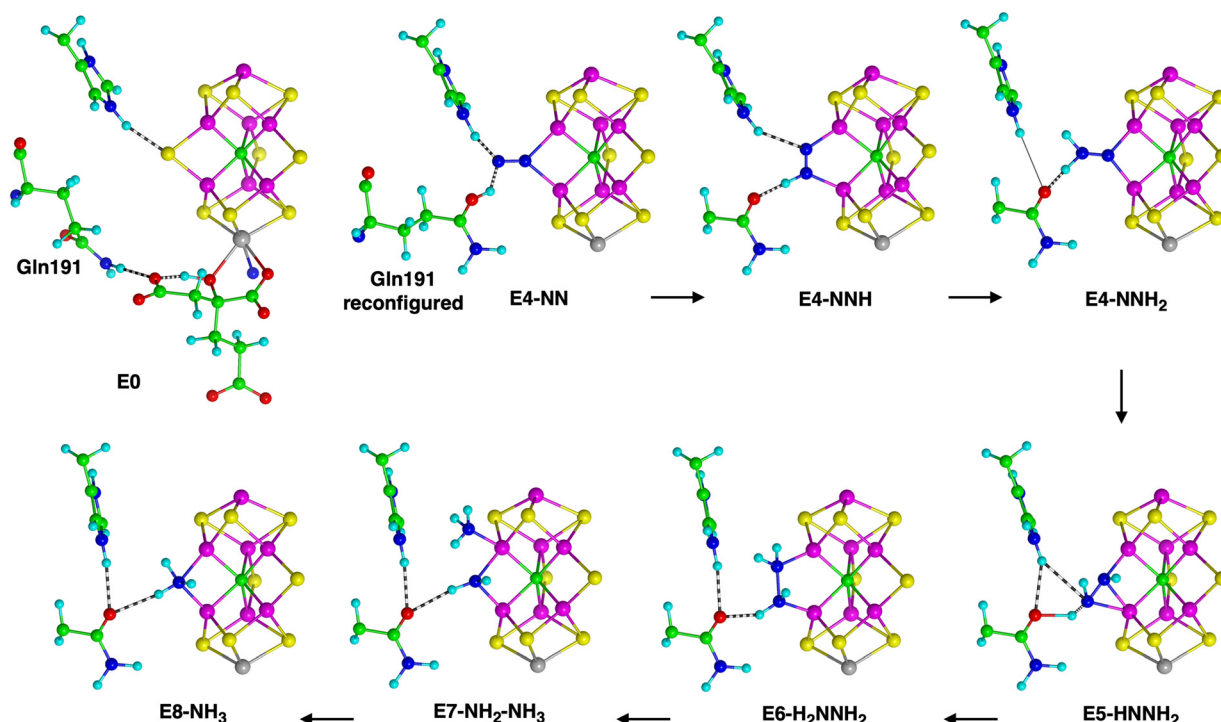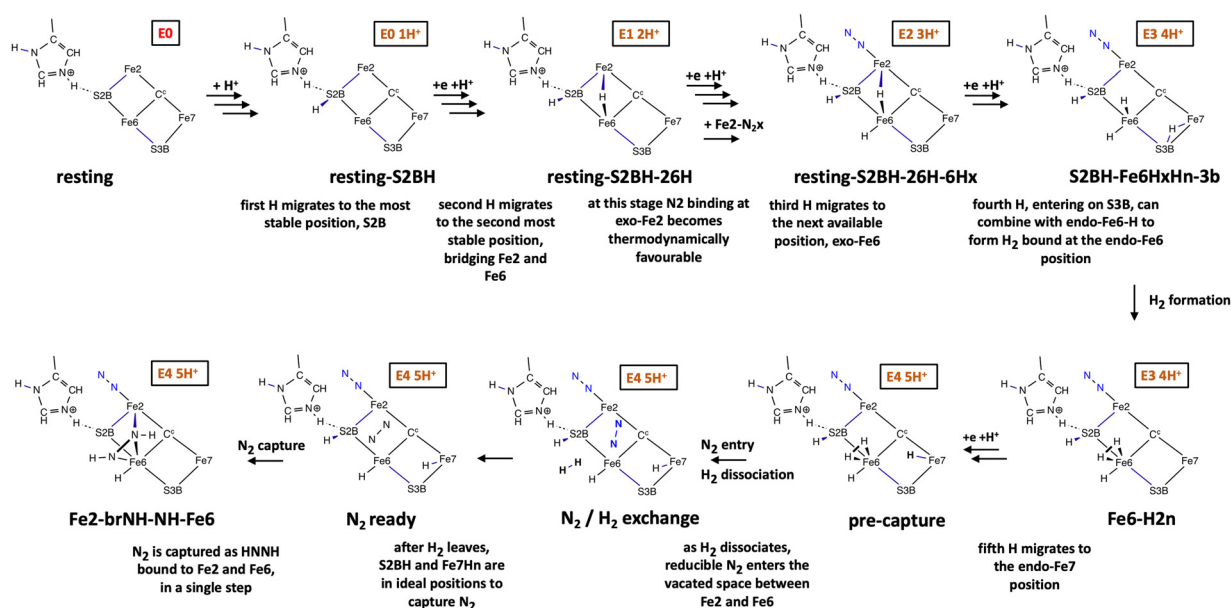
Fig. 7 Intermediates calculated by Cao and Ryde[64] with the sidechain of Gln191 flipped from the resting state E0, and S2B absent. The structures pictured were generated from Fig. 8 in ref. 64: coordinates are not available. In E4−NN there is irregular protonation of Gln191 sidechain CO. In E4−NNH$_2$ the hydrogen bond from His195NεH is too long.

Scheme 1 Skeletons and labels of the main intermediates in the first section of the mechanism, including H$_2$ formation, H$_2$/N$_2$ exchange, and N$_2$ capture to generate bound HNNH. The numbers of electrons and protons added at each stage are shown in the status boxes. The arrow clusters indicate the sequence of steps in each of which a proton is introduced from the proton supply chain[81] onto S3B, probably triggered by the entry of an electron,[80] and migrates to other sites on FeMo-co. N$_2$ occasionally bound at the *exo* position of Fe2 is non-reducible.[79] 'br' signifies bridging.

Fe6. A different N$_2$ molecule is the one to be reduced ('reducible N$_2$'), entering at the intermediate **N2/H2 exchange** in Scheme 1.

Scheme 1 encompasses many significant aspects of the early stages of the mechanism: (1) the formation of H$_2$, (2) introduction of reducible N$_2$, (3) the H$_2$/N$_2$ exchange, (4)

capture of reducible N_2 by H atoms on S2B and *endo*-Fe7, and (5) formation of bound HNNH. The exergonic N_2 capture reaction, from **N2-ready** to **Fe2–brNH–NH–Fe6**, is single step, with concerted formation of two H–N bonds and three N–Fe bonds, and reaction barrier 26–29 kcal mol^{-1} (depending on electronic state).[76]

How does all this happen with S2B intact? Fig. 8 shows actual geometries calculated for the intermediates and one key transition state: His195 and its significant hydrogen bond to S2B are included on the pictures. Notable properties are: (1) at **N2-ready**, H atoms on S2B and at *endo*-Fe7 are stereochemically propitious for transfer to the two N atoms on incoming

reducible N_2; (2) at **transition state** there is concerted formation of two H–N bonds and three N–Fe bonds, with regular stereochemistry at all atoms undergoing changes; (3) the coordination stereochemistry at Fe2 is always regular, being octahedral in **resting-S2BH–26H–6Hx** and **Fe2–brNH–NH–Fe6** and standard trigonal bipyramidal in the other intermediates; (4) the coordination stereochemistry at Fe6 is octahedral or close to octahedral in all intermediates except during the dissociative H_2/N_2 exchange; (5) elongation of Fe6–C^c ranges 2.25 to 2.47 Å, and occurs when Fe6 is fully ligated. The reaction trajectory for the crucial N_2 capture step was analysed in detail to assess the possible occurrence of H atom tunneling.[76]

(a)

(b)
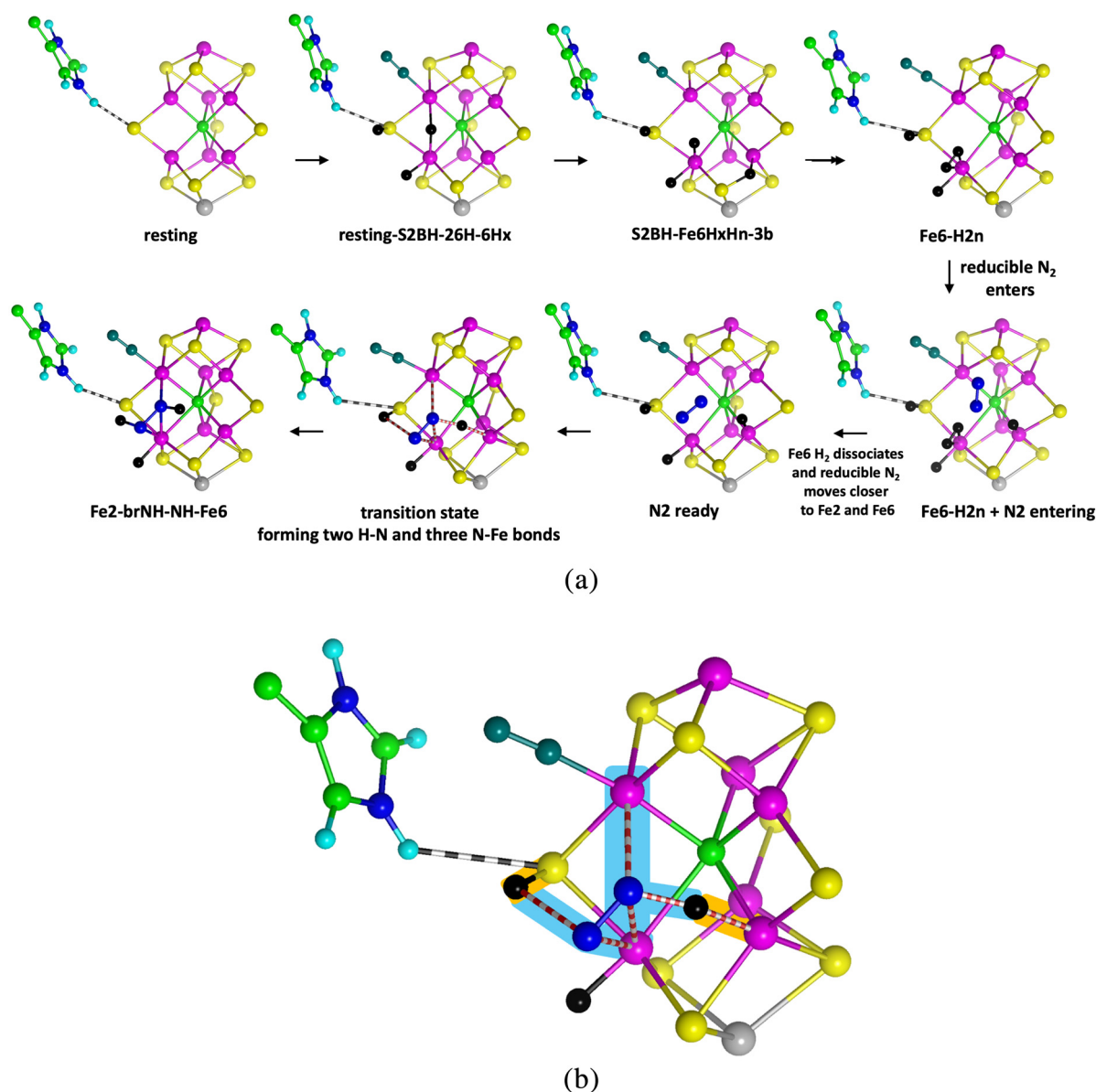
Fig. 8   (a) Calculated geometries of intermediates and of the transition state for N_2 capture (bonds breaking and making are red-white striped). Key H atoms are black. The side chain of His195 is included, with the Nε-H → S2B hydrogen bond. Elongated C^c–Fe6 distances are 2.31 Å in **Fe6–H2n**, 2.47 Å in **Fe6–H2n + N2 entering**, 2.25 Å in **N2 ready**, 2.38 Å in **Fe2–brNH–NH–Fe6**. (b) Enlarged picture of the transition state for N_2 capture, emphasising the two bonds being broken (orange) and the five bonds being formed (blue).

The key role of S2B in maintaining regular coordination of Fe2 and Fe6 and in provision of H to N is obvious. Significantly, the H atom on S2B is ideally located to transfer to N, as shown (Fig. 8) in the geometries in the sequence **N2 ready → transition state → Fe2–brNH–NH–Fe6**.

The second section of the complete mechanism is outlined in Scheme 2. This is a simplified version of Scheme 7 of ref. 78 which contains all details. In this part of the mechanism there are four types of reaction step: (1) transfer of H from His195 NεH to S2B; (2) introduction and migration of the sixth H atom followed by transfer to N forming bound H$_2$NNH; (3) N–N bond breaking with concomitant formation of NH$_3$ bound to Fe6; (4) dissociation of NH$_3$. Overall the electron/proton status changes from E4 5H$^+$ to E6 6H$^+$, and, as marked on Scheme 2, results are available for e$^-$ H$^+$ additions occurring at different stages. The calculated reaction energy

profiles for these steps[78] show that all except one, the N–N breaking step, have small reaction barriers. The N–N breaking step is exergonic by 30 to 42 kcal mol^{-1}, with kinetic barriers ranging 27 to 35 kcal mol^{-1}. This N–N breaking is proposed to be the slow step identified in the kinetic analysis of Harris *et al.*,[87] occurring after formation of the HNNH intermediate. It is remarkable that the H transfer from His195 to S2B is exergonic by 5 to 14 kcal mol^{-1}, with small kinetic barriers ranging 1 to 8 kcal mol^{-1}. As a consequence, the final intermediate in this reaction sequence, **Fe2–brNH–Fe6–S2BH**, has H restored to S2B and is primed for the next phase of the mechanism.

Two aspects of the geometries of the intermediates are notable in the present context. One is that the intermediate **Fe2–brNH–NH2–Fe6Hx** has ideal geometry for N–N breaking. Fig. 9 illustrates how 6Hx, Fe6, and the two N atoms are essen-
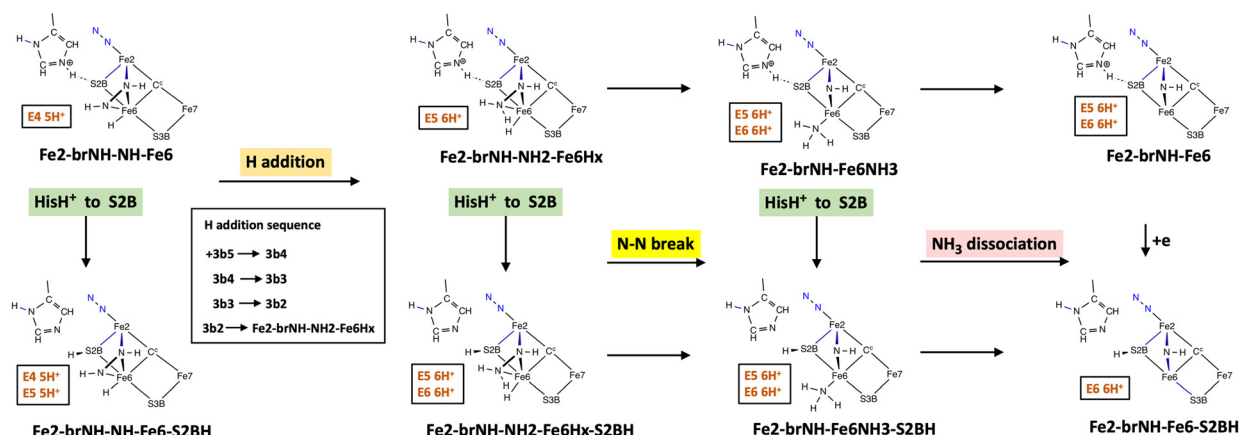
Scheme 2 . Reaction pathways that break the N–N bond and then form and release NH$_3$.[78] Some intermediates and reaction steps were calculated with alternative electron populations, as marked in the status boxes.
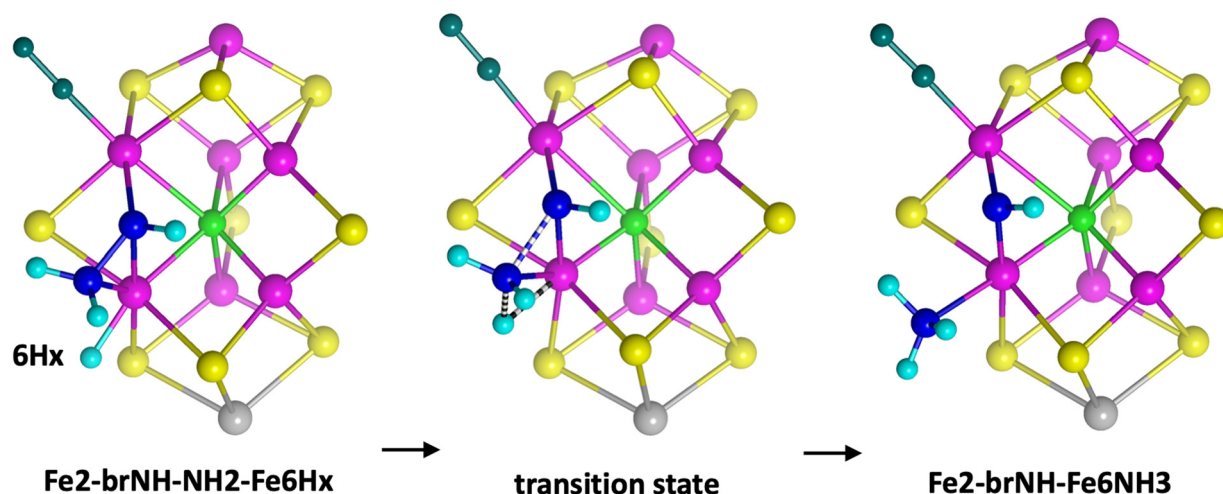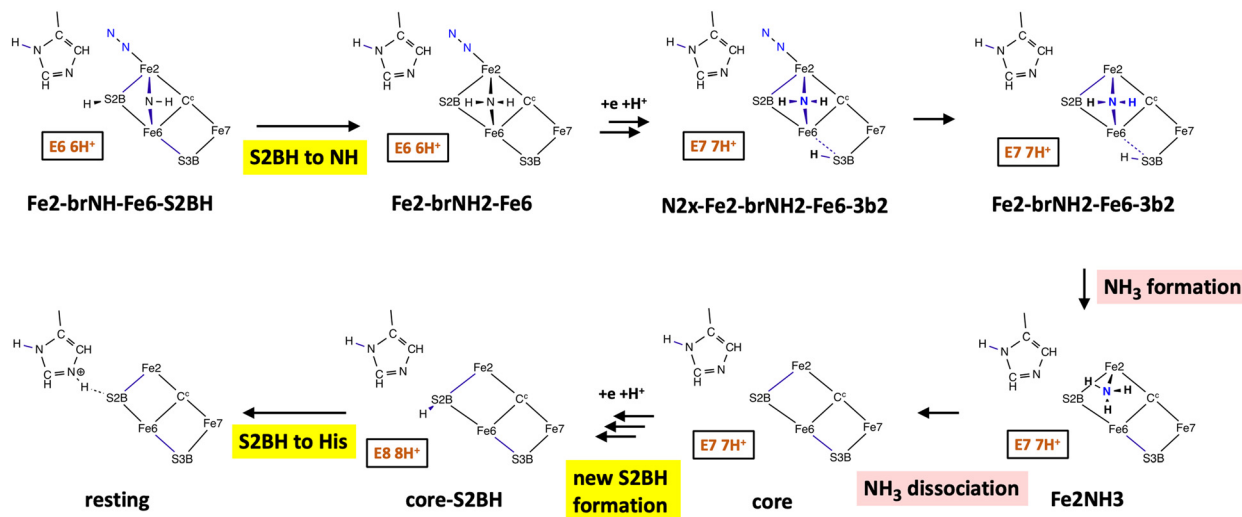

Fig. 9 Geometrical characteristics of the reaction step that breaks N–N and forms NH$_3$. The Fe2–NH–Fe6 bridge is maintained throughout, together with the Fe2–S2B–Fe6 bridge. Note how 6Hx, Fe6, the two N atoms, and C^c are essentially coplanar. N–N extends from 1.38 Å to 1.71 Å at the transition state, and the NH$_2$ group undergoes a standard inversion through the transition state.

Scheme 3 The steps in which S2B is an active reagent are highlighted yellow.

tially coplanar, and remain so during the transition as N···N elongates, H–N forms, H–Fe6 separates, and NH_3 is generated. This reaction is inversion of the NH_2 group as it separates from N and forms NH_3. Secondly, S2B, as a bridge between Fe2 and Fe6 in all intermediates, completes the favourable octahedral coordination of Fe2 and Fe6. The favourable geometry of the conversion shown in Fig. 9 depends on the presence of S2B.

The final stage of the mechanism[77] is outlined in Scheme 3. First, S2BH generated in the previous stage converts bridging NH to bridging NH_2. Then another H is introduced at S3B, from which it transfers to the NH_2 bridge to generate NH_3 coordinated at the *endo* position of Fe2. After dissociation of this second NH_3 the bare core of FeMo-co remains. The eighth proton (plus electron) enters and migrates to S2B which is the most stable location for H on FeMo-co.[48,82,88] Transfer of this H from S2B to His195 regenerates the resting state (**core-S2BH → resting** is 8 kcal mol^{-1} exergonic with a barrier of 4 kcal mol^{-1}). A complete analysis of the thermodynamics of the steps in Scheme 3 is provided in ref. 77. Note that, as in all previous steps, S2B as a bridge between Fe2 and Fe6 is an essential component, maintaining favourable coordination stereochemistry at Fe2 and Fe6. The yellow highlights in Scheme 3 draw attention to S2B also functioning as active reagent.

Overall, intact S2B has five direct mechanistic roles: (1) H transfer from S2B to N in the N_2 capture step (**N2 ready → Fe2–brNH–NH–Fe6**); (2) recovery of S2BH from His195NεH in the sequence forming **Fe2–brNH–Fe6–S2BH**; (3) H transfer from S2B to N to form **Fe2–brNH2–Fe6**; (4) formation of S2BH after introduction of the eighth H; (5) H transfer from S2BH to recover the **resting** state.

This 21 step chemical choreography of the complete mechanism conserves the structure of FeMo-co. No bonds in the cofactor are broken. The plasticity of FeMo-co is manifest in the usual extensions of the C^c–Fe bonds caused by *exo*-Fe ligation. Homocitrate does not change its coordination geometry,

as is required by the critical role of homocitrate in controlling the proton wire,[56,81] and homocitrate involvement in the first steps for egress of NH_3.[89] The mechanism is chemically conservative in the sense that none of the bond making and bond breaking steps is unusual. Standard stereochemistry is maintained at all atoms throughout the mechanism. The mechanism deploys the geometry of FeMo-co – particularly the Fe2, Fe6, S2B, S3B, Fe7 segment, together with His195 – to achieve propitious geometry for the reaction steps. All eight protons required in the enzyme cycle are introduced from the protein surface along a conserved proton wire terminating at S3B.[81,90] The concerted formation of five bonds in the N_2 capture single step is distinctive and unique, and uses straightforward conventional chemistry. Other attributes, elaborated in the primary publications, are the estimation of entropy contributions, the analysis of reaction trajectories to assess possibilities of H atom quantum tunneling, and the interpretation of the slow step identified in the recent description of steady state enzyme kinetics[87] as the N–N breaking step shown in Fig. 9.

This conservative mechanism is based on the architecture and function of FeMo-co and the protein surrounding the active site.[56] These are pictured in Fig. 10. More specifically, the functional components of the proposed mechanism are cartooned in Fig. 11. The hydrogenation zone is between Fe2, S2B, Fe6, S3B and Fe7, and the various H atoms required there are provided by S2B, Fe6, S3B and Fe7.

Other computational investigations of mechanism describe limited aspects, being mainly sequences of calculated intermediates. However, Ryde and coworkers describe mechanisms in which most pathways involve transfer of a proton from S2B to the substrate.[66] This paper is the only other one that includes description of the source and pathways for incoming protons. This paper also describes calculated reaction barriers, which are absent from almost all of the other reports.
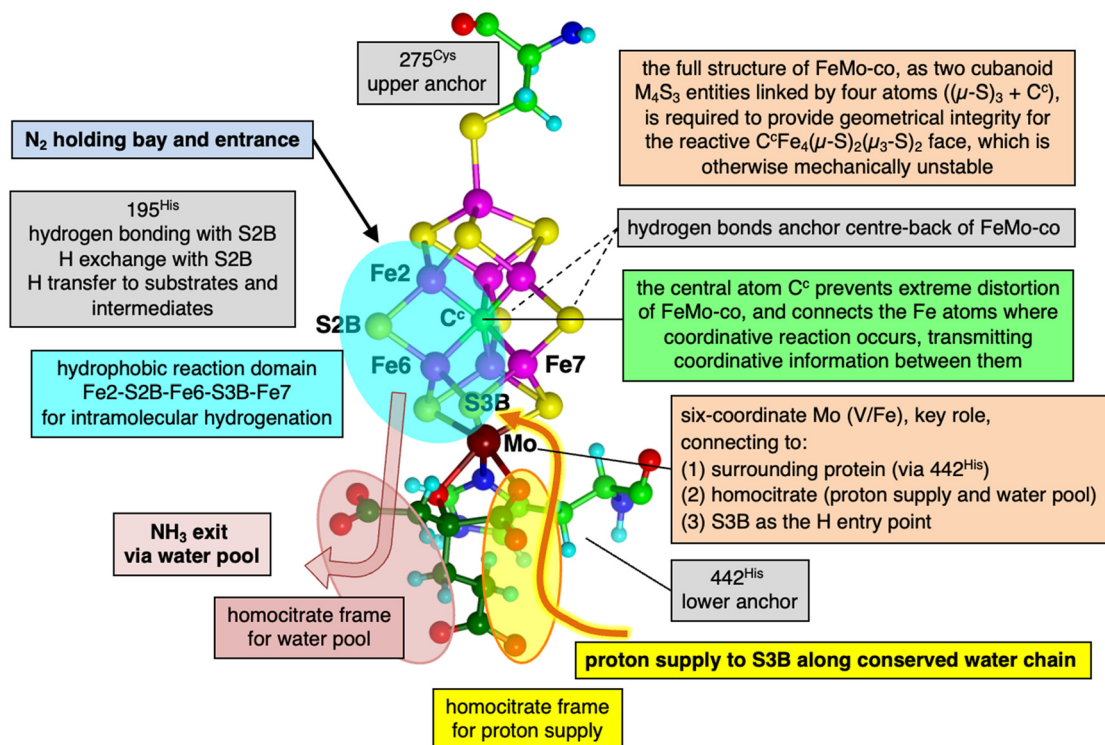
Fig. 10 Structural components of the nitrogenase active site, and their mechanistic roles supporting the conservative mechanism. Reproduced from ref. 77.
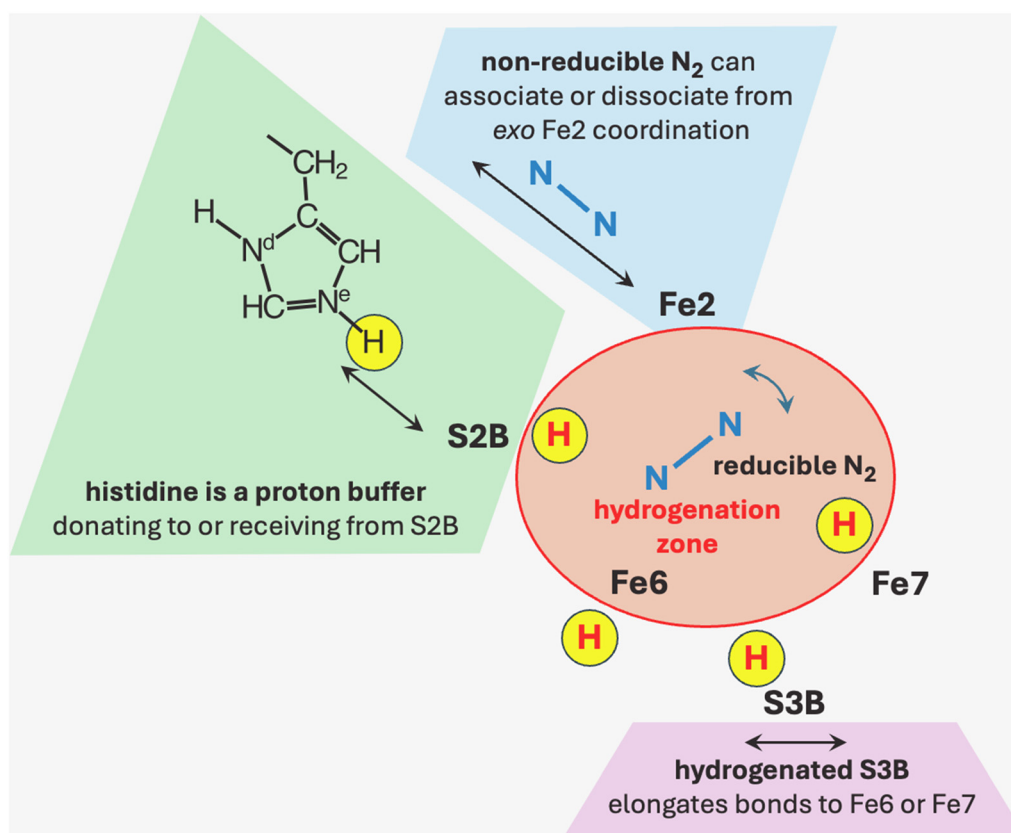

Fig. 11 Functional components of the nitrogenase mechanism. The four red H atom sites, S2B H, *exo*-Fe6-H, S3B−H and *endo*-Fe7−H, effect the intramolecular hydrogenation of N_2 and of subsequent intermediates in the hydrogenation zone. Reproduced from ref. 77.

7 Dilemma

Now we have the dilemma: does nitrogenase use a disruptive mechanism or a conservative mechanism? Disruptive mechanisms, derived from many experiments, are still largely conceptual with many uncertain components. Details of the intermediates and steps after displacement of S2B are still to be elaborated experimentally for physiological catalysis. These disruptive mechanisms are challenged by a complete and geometrically competent mechanism that retains bridging S2B as a crucial component. Will S2B flee or contribute? Shakespeare's Hamlet wondered "To be, or not to be, that is the question" (Act III Scene 1). We can be more analytical about "S2B or not S2B?" and I have assembled the evidence in this Perspective.

The experiment – theory dichotomy also underlies this dilemma. The disruptive mechanism ideas are based on experimental results, whereas the conservative mechanism is derived from computational simulation. Experiments, partly *in vivo* and partly *in vitro*, are challenged by *in silico* information. What are the prospects for resolution? It is unfortunate that experimentation to reveal the many intermediates in the nitrogenase reaction cycle faces multiple difficulties.

A natural philosopher might ask "Why would evolution select a more complex mechanism with disruptive dissociation and re-association of S2B when a more straightforward pathway could be available?"

Conflicts of interest

There are no conflicts to declare.

Data availability

There is no additional data.

Acknowledgements

References

1 V. Smil, *Enriching the Earth: Fritz Haber, Carl Bosch, and the Transformation of World Food Production*, MIT Press, Cambridge, Massachusetts, 2001.

2 A. K. Garcia, D. F. Harris, A. J. Rivier, B. M. Carruthers, A. Pinochet-Barros, L. C. Seefeldt and B. Kaçar, Nitrogenase resurrection and the evolution of a singular enzymatic mechanism, *eLife*, 2023, **12**, e85003, DOI: 10.7554/eLife.85003.

3 O. Einsle and D. C. Rees, Structural Enzymology of Nitrogenase Enzymes, *Chem. Rev.*, 2020, **120**, 4969–5004, DOI: 10.1021/acs.chemrev.0c00067.

4 S. D. Threatt and D. C. Rees, Biological nitrogen fixation in theory, practice, and reality: a perspective on the molybdenum nitrogenase system, *FEBS Lett.*, 2022, **597**, 45–58, DOI: 10.1002/1873-3468.14534.

5 H. Schindelin, C. Kisker, J. L. Schlessman, J. B. Howard and D. C. Rees, Structure of ADP-AlF$_4^-$ stabilized nitrogenase complex and its implications for signal transduction, *Nature*, 1997, **387**, 370–376.

6 C. H. Kim, W. E. Newton and D. R. Dean, Role of the MoFe protein alpha subunit histidine-195 residue in FeMo-cofactor binding and nitrogenase catalysis, *Biochemistry*, 1995, **34**, 2798–2808.

7 M. J. Dilworth, K. Fisher, C. H. Kim and W. E. Newton, Effects on substrate reduction of substitution of histidine-195 by glutamine in the alpha-subunit of the MoFe protein of Azotobacter vinelandii nitrogenase, *Biochemistry*, 1998, **37**, 17495–17505.

8 K. Fisher, M. J. Dilworth and W. E. Newton, Differential Effects on N$_2$ Binding and Reduction, HD Formation, and Azide Reduction with α-195His- and α-191Gln-Substituted MoFe Proteins of Azotobacter Vinelandii Nitrogenase, *Biochemistry*, 2000, **39**, 15570–15577.

9 B. M. Barney, H.-I. Lee, P. C. Dos Santos, B. M. Hoffman, D. R. Dean and L. C. Seefeldt, Breaking the N$_2$ triple bond: insights into the nitrogenase mechanism, *Dalton Trans.*, 2006, 2277–2284, DOI: 10.1039/b517633f.

10 P. C. Dos Santos, S. M. Mayer, B. M. Barney, L. C. Seefeldt and D. R. Dean, Alkyne substrate interaction within the nitrogenase MoFe protein, *J. Inorg. Biochem.*, 2007, **101**, 1642–1648.

11 L. C. Seefeldt, B. M. Hoffman and D. R. Dean, Mechanism of Mo-Dependent Nitrogenase, *Annu. Rev. Biochem.*, 2009, **78**, 701–722.

12 R. Sarma, B. M. Barney, S. Keable, D. R. Dean, L. C. Seefeldt and J. W. Peters, Insights into substrate binding at FeMo-cofactor in nitrogenase from the structure of an α-70Ile MoFe protein variant, *J. Inorg. Biochem.*, 2010, **104**, 385–389.

13 S. M. Keable, J. Vertemara, O. A. Zadvornyy, B. J. Eilers, K. Danyal, A. J. Rasmussen, L. De Gioia, G. Zampella, L. C. Seefeldt and J. W. Peters, Structural characterization of the nitrogenase molybdenum-iron protein with the substrate acetylene trapped near the active site, *J. Inorg. Biochem.*, 2018, **180**, 129–134, DOI: 10.1016/j.jinorgbio.2017.12.008.

14 Z. Maskos, K. Fisher, M. Sorlie, W. E. Newton and B. J. Hales, Variant MoFe proteins of Azotobacter vinelandii: effects of carbon monoxide on electron paramagnetic resonance spectra generated during enzyme turnover, *J. Biol. Inorg. Chem.*, 2005, **10**, 394–406.

15 P. M. C. Benton, J. Christiansen, D. R. Dean and L. C. Seefeldt, Stereospecificity of Acetylene Reduction Catalyzed by Nitrogenase, *J. Am. Chem. Soc.*, 2001, **123**, 1822–1827.

16 P. C. Dos Santos, R. Igarashi, H.-I. Lee, B. M. Hoffman, L. C. Seefeldt and D. R. Dean, Substrate Interactions with the Nitrogenase Active Site, *Acc. Chem. Res.*, 2005, **38**, 208–214.

17 R. N. F. Thorneley and D. J. Lowe, in *Molybdenum enzymes*, ed. T. G. Spiro, Wiley Interscience, New York, 1985, ch. 5, pp. 221–284.

18 R. N. F. Thorneley and D. J. Lowe, Nitrogenase - Substrate Binding and Activation, *J. Biol. Inorg. Chem.*, 1996, **1**, 576–580.

19 J. Kim and D. C. Rees, Crystallographic structure and functional implications of the nitrogenase molybdenum-iron protein from Azotobacter vinelandii, *Nature*, 1992, **360**, 553–560.

20 T. Spatzal, M. Aksoyoglu, L. Zhang, S. L. A. Andrade, E. Schleicher, S. Weber, D. C. Rees and O. Einsle, Evidence for Interstitial Carbon in Nitrogenase FeMo Cofactor, *Science*, 2011, **334**, 940, DOI: 10.1126/science.1214025.

21 T. Spatzal, K. A. Perez, O. Einsle, J. B. Howard and D. C. Rees, Ligand binding to the FeMo-cofactor: Structures of CO-bound and reactivated nitrogenase, *Science*, 2014, **345**, 1620–1623, DOI: 10.1126/science.1256679.

22 T. Spatzal, K. A. Perez, J. B. Howard and D. C. Rees, Catalysis-dependent selenium incorporation and migration in the nitrogenase active site iron-molybdenum cofactor, *eLife*, 2015, **4**, e11620, DOI: 10.7554/eLife.11620.

23 I. Dance, Mechanisms of the S/CO/Se interchange reactions at FeMo-co, the active site cluster of nitrogenase, *Dalton Trans.*, 2016, **45**, 14285–14300, DOI: 10.1039/C6DT03159E.

24 D. Sippel and O. Einsle, The structure of vanadium nitrogenase reveals an unusual bridging ligand, *Nat. Chem. Biol.*, 2017, **13**, 956–960, DOI: 10.1038/nchembio.2428.

25 D. Sippel, M. Rohde, J. Netzer, C. Trncik, J. Gies, K. Grunau, I. Djurdjevic, L. Decamps, S. L. A. Andrade and O. Einsle, A bound reaction intermediate sheds light on the mechanism of nitrogenase, *Science*, 2018, **359**, 1484–1489, DOI: 10.1126/science.aar2765.

26 B. Benediktsson, A. T. Thorhallsson and R. Bjornsson, QM/MM calculations reveal a bridging hydroxo group in a vanadium nitrogenase crystal structure, *Chem. Commun.*, 2018, **54**, 7310–7313, DOI: 10.1039/C8CC03793K.

27 L. Cao, O. Caldararu and U. Ryde, Does the crystal structure of vanadium nitrogenase contain a reaction intermediate? Evidence from quantum refinement, *J. Biol. Inorg. Chem.*, 2020, **25**, 847–861, DOI: 10.1007/s00775-020-01813-z.

28 M. Rohde, K. Grunau and O. Einsle, CO Binding to the FeV Cofactor of CO-Reducing Vanadium Nitrogenase at Atomic Resolution, *Angew. Chem., Int. Ed.*, 2020, **59**, 23626–23630, DOI: 10.1002/anie.202010790.

29 T. M. Buscagan, K. A. Perez, A. O. Maggiolo, D. C. Rees and T. Spatzal, Structural Characterization of Two CO Molecules Bound to the Nitrogenase Active Site, *Angew. Chem., Int. Ed.*, 2021, **60**, 5704–5707, DOI: 10.1002/anie.202015751.

30 M. Rohde, K. Laun, I. Zebger, S. T. Stripp and O. Einsle, Two ligand-binding sites in CO-reducing V nitrogenase

31 W. Kang, C. C. Lee, A. J. Jasniewski, M. W. Ribbe and Y. Hu, Structural evidence for a dynamic metallocofactor during N$_2$ reduction by Mo-nitrogenase, *Science*, 2020, **368**, 1381–1385, DOI: 10.1126/science.aaz6748.

32 J. W. Peters, O. Einsle, D. R. Dean, S. DeBeer, B. M. Hoffman, P. L. Holland and L. C. Seefeldt, Comment on "Structural evidence for a dynamic metallocofactor during N$_2$ reduction by Mo-nitrogenase", *Science*, 2021, **371**, abe5481, DOI: 10.1126/science.abe5481.

33 W. Kang, C. C. Lee, A. J. Jasniewski, M. W. Ribbe and Y. Hu, Response to Comment on "Structural evidence for a dynamic metallocofactor during N$_2$ reduction by Mo-nitrogenase", *Science*, 2021, **371**, eabe5856, DOI: 10.1126/science.abe5856.

34 J. Bergmann, E. Oksanen and U. Ryde, Critical evaluation of a crystal structure of nitrogenase with bound N$_2$ ligands, *J. Biol. Inorg. Chem.*, 2021, **26**, 341–353, DOI: 10.1007/s00775-021-01858-8.

35 C. C. Lee, W. Kang, A. J. Jasniewski, M. T. Stiebritz, K. Tanifuji, M. W. Ribbe and Y. Hu, Evidence of substrate binding and product release via belt-sulfur mobilization of the nitrogenase cofactor, *Nat. Catal.*, 2022, **5**, 443–454, DOI: 10.1038/s41929-022-00782-7.

36 C. C. Lee, M. Stang, M. W. Ribbe and Y. Hu, ATP-Independent Turnover of Dinitrogen Intermediates Captured on the Nitrogenase Cofactor, *Angew. Chem., Int. Ed.*, 2024, e202400273, DOI: 10.1002/anie.202400273.

37 C. C. Lee, K. Chatterjee, J. Yano, J. Kern, M. T. Stiebritz, M. W. Ribbe and Y. Hu, Belt-sulfur mobilization as a crucial mechanistic feature shared between the vanadium and molybdenum nitrogenases, *Chem. Catal.*, 2025, **5**, 101366, DOI: 10.1016/j.checat.2025.101366.

38 C. Trncik, F. Detemple and O. Einsle, Iron-only Fe-nitrogenase underscores common catalytic principles in biological nitrogen fixation, *Nat. Catal.*, 2023, **6**, 415–424, DOI: 10.1038/s41929-023-00952-1.

39 D. P. Klebl, M. S. C. Gravett, D. Kontziampasis, D. J. Wright, R. S. Bon, D. C. F. Monteiro, M. Trebbin, F. Sobott, H. D. White, M. C. Darrow, R. F. Thompson and S. P. Muench, Need for Speed: Examining Protein Behavior during CryoEM Grid Preparation at Different Timescales, *Structure*, 2020, **28**, 1238–1248, DOI: 10.1016/j.str.2020.07.018.

40 D. P. Klebl, L. Aspinall and S. P. Muench, Time resolved applications for Cryo-EM; approaches, challenges and future directions, *Curr. Opin. Struct. Biol.*, 2023, **83**, 102696, DOI: 10.1016/j.sbi.2023.102696.

41 H. L. Rutledge, B. D. Cook, H. P. M. Nguyen, M. A. Herzik and F. A. Tezcan, Structures of the nitrogenase complex prepared under catalytic turnover conditions, *Science*, 2022, **377**, 865–869, DOI: 10.1126/science.abq7641.

42 R. A. Warmack, B. B. Wenke, T. Spatzal and D. C. Rees, Anaerobic cryoEM protocols for air-sensitive nitrogenase

proteins, *Nat. Protoc.*, 2024, **19**, 2026–2051, DOI: 10.1038/s41596-024-00973-5.

43 R. A. Warmack and D. C. Rees, Nitrogenase beyond the Resting State: A Structural Perspective, *Molecules*, 2023, **28**, 7952, DOI: 10.3390/molecules28247952.

44 R. A. Warmack and D. C. Rees, Structural evolution of nitrogenase states under alkaline turnover, *Nat. Commun.*, 2024, **15**, 10472, DOI: 10.1038/s41467-024-54713-0.

45 P. E. Doan, J. Telser, B. M. Barney, R. Y. Igarashi, D. R. Dean, L. C. Seefeldt and B. M. Hoffman, 57Fe ENDOR Spectroscopy and 'Electron Inventory' Analysis of the Nitrogenase E4 Intermediate Suggest the Metal-Ion Core of FeMo-Cofactor Cycles Through Only One Redox Couple, *J. Am. Chem. Soc.*, 2011, **133**, 17329–17340.

46 V. Hoeke, L. Tociu, D. A. Case, L. C. Seefeldt, S. Raugei and B. M. Hoffman, High-Resolution ENDOR Spectroscopy Combined with Quantum Chemical Calculations Reveals the Structure of Nitrogenase Janus Intermediate E4(4H), *J. Am. Chem. Soc.*, 2019, **141**, 11984–11996, DOI: 10.1021/jacs.9b04474.

47 A. T. Thorhallsson, B. Benediktsson and R. Bjornsson, A model for dinitrogen binding in the E4 state of nitrogenase, *Chem. Sci.*, 2019, **10**, 11110–11124, DOI: 10.1039/C9SC03610E.

48 I. Dance, Survey of the geometric and electronic structures of the key hydrogenated forms of FeMo-co, the active site of the enzyme nitrogenase: principles of the mechanistically significant coordination chemistry, *Inorganics*, 2019, **7**, 8, DOI: 10.3390/inorganics7010008.

49 S. Raugei, L. C. Seefeldt and B. M. Hoffman, Critical computational analysis illuminates the reductive-elimination mechanism that activates nitrogenase for N₂ reduction, *Proc. Natl. Acad. Sci. U. S. A.*, 2018, **115**, E10521–E10530, DOI: 10.1073/pnas.1810211115.

50 K. Sengupta, J. P. Joyce, L. Decamps, L. Kang, R. Bjornsson, O. Rüdiger and S. DeBeer, Investigating the Molybdenum Nitrogenase Mechanistic Cycle Using Spectroelectrochemistry, *J. Am. Chem. Soc.*, 2025, **147**, 2099–2114, DOI: 10.1021/jacs.4c16047.

51 M. W. Ribbe and Y. Hu, Belt-sulfur mobilization in nitrogenase biosynthesis and catalysis, *Trends Chem.*, 2023, **5**, 108–111, DOI: 10.1016/j.trechm.2022.12.001.

52 O. Einsle, Catalysis and structure of nitrogenases, *Curr. Opin. Struct. Biol.*, 2023, **83**, 102719, DOI: 10.1016/j.sbi.2023.102719.

53 T. Spatzal, K. A. Perez, O. Einsle, J. B. Howard and D. C. Rees, Ligand binding to the FeMo-cofactor: Structures of CO-bound and reactivated nitrogenase, *Science*, 2014, **345**, 1620.

54 R. A. Warmack and D. C. Rees, The nitrogenase mechanism: new roles for the dangler?, *J. Biol. Inorg. Chem.*, 2025, **30**, 125–133, DOI: 10.1007/s00775-024-02085-7.

55 J. B. Varley, Y. Wang, K. Chan, F. Studt and J. K. Norskov, Mechanistic insights into nitrogen fixation by nitrogenase enzymes, *Phys. Chem. Chem. Phys.*, 2015, **17**, 29541–29557, DOI: 10.1039/C5CP04034E.

56 I. Dance, Deserts, Rivers, Pools and Billabongs: Water Features of the Nitrogenase Proteins, and their Functions, *ChemBioChem*, 2025, e202500541, DOI: 10.1002/cbic.202500541.

57 H. Jiang and U. Ryde, Thermodynamically Favourable States in the Reaction of Nitrogenase without Dissociation of any Sulfide Ligand, *Chem. – Eur. J.*, 2022, **28**, e202103933, DOI: 10.1002/chem.202103933.

58 L. Cao and U. Ryde, N₂H₂ binding to the nitrogenase FeMo cluster studied by QM/MM methods, *J. Biol. Inorg. Chem.*, 2020, **25**, 521–540, DOI: 10.1007/s00775-020-01780-5.

59 I. Dance, Structures and reaction dynamics of N₂ and H₂ binding at FeMo-co, the active site of nitrogenase, *Dalton Trans.*, 2021, **50**, 18212–18237, DOI: 10.1039/d1dt03548g.

60 I. Dance, The binding of reducible N₂ in the reaction domain of nitrogenase, *Dalton Trans.*, 2023, **52**, 2013–2026, DOI: 10.1039/D2DT03599E.

61 I. Dance, How feasible is the reversible S-dissociation mechanism for the activation of FeMo-co, the catalytic site of nitrogenase?, *Dalton Trans.*, 2019, **48**, 1251–1262, DOI: 10.1039/c8dt04531c.

62 I. Dance, Understanding the tethered unhooking and rehooking of S2B in the reaction domain of FeMo-co, the active site of nitrogenase, *Dalton Trans.*, 2022, **51**, 15538–15554, DOI: 10.1039/D2DT02571J.

63 H. Jiang, O. K. G. Svensson and U. Ryde, QM/MM Study of Partial Dissociation of S2B for the E2 Intermediate of Nitrogenase, *Inorg. Chem.*, 2022, **61**, 18067–18076, DOI: 10.1021/acs.inorgchem.2c02488.

64 L. Cao and U. Ryde, Putative reaction mechanism of nitrogenase after dissociation of a sulfide ligand, *J. Catal.*, 2020, **391**, 247–259, DOI: 10.1016/j.jcat.2020.08.028.

65 W. J. Wei and P. E. M. Siegbahn, A Mechanism for Nitrogenase Including Loss of a Sulfide, *Chemistry*, 2022, **28**, e202103745, DOI: 10.1002/chem.202103745.

66 H. Jiang, O. K. G. Svensson, L. Cao and U. Ryde, Proton Transfer Pathways in Nitrogenase with and without Dissociated S2B, *Angew. Chem., Int. Ed.*, 2022, **61**, e202208544, DOI: 10.1002/anie.202208544.

67 H. Jiang and U. Ryde, N₂ binding to the E0–E4 states of nitrogenase, *Dalton Trans.*, 2023, **52**, 9104–9120, DOI: 10.1039/D3DT00648D.

68 Y. Pang and R. Bjornsson, Understanding the Electronic Structure Basis for N₂ Binding to FeMoco: A Systematic Quantum Mechanics/Molecular Mechanics Investigation, *Inorg. Chem.*, 2023, **62**, 5357–5375, DOI: 10.1021/acs.inorgchem.2c03967.

69 J. Kastner and P. E. Blochl, Ammonia Production at the FeMo Cofactor of Nitrogenase: Results from Density Functional Theory, *J. Am. Chem. Soc.*, 2007, **129**, 2998–3006.

70 I. Dance, Computational Investigations of the Chemical Mechanism of the Enzyme Nitrogenase, *ChemBioChem*, 2020, **21**, 1671–1709, DOI: 10.1002/cbic.201900636.

71 P. P. Hallmen and J. Kästner, N₂ Binding to the FeMo-Cofactor of Nitrogenase, *Z. Anorg. Allg. Chem.*, 2015, **641**, 118–122, DOI: 10.1002/zaac.201400114.

72 L. Cao and U. Ryde, What Is the Structure of the E4 Intermediate in Nitrogenase?, *J. Chem. Theory Comput.*, 2020, **16**, 1936–1952, DOI: 10.1021/acs.jctc.9b01254.

73 R. Y. Igarashi, M. Laryukhin, P. C. Dos Santos, H.-I. Lee, D. R. Dean, L. C. Seefeldt and B. M. Hoffman, Trapping H^- Bound to the Nitrogenase FeMo-cofactor Active Site During H_2 Evolution: Characterization by ENDOR Spectroscopy, *J. Am. Chem. Soc.*, 2005, **127**, 6231–6241.

74 H. Jiang and U. Ryde, Putative reaction mechanism of nitrogenase with a half-dissociated S2B ligand, *Dalton Trans.*, 2024, **53**, 11500–11513, DOI: 10.1039/D4DT00937A.

75 P. E. M. Siegbahn, Sulfide release and rebinding in the mechanism for nitrogenase, *J. Comput. Chem.*, 2024, **45**, 2835–2841, DOI: 10.1002/jcc.27494.

76 I. Dance, The activating capture of N_2 at the active site of Mo–nitrogenase, *Dalton Trans.*, 2024, **53**, 14193–14211, DOI: 10.1039/d4dt01866d.

77 I. Dance, The Mechanism of Nitrogenase: formation and release of the second NH_3 and completion of the cycle, *Dalton Trans.*, 2025, **54**, 9877–9900, DOI: 10.1039/d5dt00658a.

78 I. Dance, The mechanism of Mo-nitrogenase: from N_2 capture to first release of NH_3, *Dalton Trans.*, 2024, **53**, 19360–19377, DOI: 10.1039/d4dt02606c.

79 I. Dance, Understanding non-reducible N_2 in the mechanism of Mo-nitrogenase, *Dalton Trans.*, 2025, **54**, 3013–3026, DOI: 10.1039/d4dt03146f.

80 I. Dance, What triggers the coupling of proton transfer and electron transfer at the active site of nitrogenase?, *Dalton Trans.*, 2024, **53**, 7996–8004, DOI: 10.1039/d4dt00474d.

81 I. Dance, The pathway for serial proton supply to the active site of nitrogenase: enhanced density functional modeling of the Grotthuss mechanism, *Dalton Trans.*, 2015, **44**, 18167–18186, DOI: 10.1039/C5DT03223G.

82 I. Dance, The stereochemistry and dynamics of the introduction of hydrogen atoms onto FeMo-co, the active site of nitrogenase, *Inorg. Chem.*, 2013, **52**, 13068–13077, DOI: 10.1021/ic401818k.

83 R. Y. Igarashi and L. C. Seefeldt, Nitrogen fixation: the mechanism of the Mo-dependent nitrogenase, *Crit. Rev. Biochem. Mol. Biol.*, 2003, **38**, 351–384, DOI: 10.1080/10409230391036766.

84 C. N. Morrison, J. A. Hoy, L. Zhang, O. Einsle and D. C. Rees, Substrate Pathways in the Nitrogenase MoFe Protein by Experimental Identification of Small Molecule Binding Sites, *Biochemistry*, 2015, **54**, 2052–2060, DOI: 10.1021/bi501313k.

85 D. Smith, K. Danyal, S. Raugei and L. C. Seefeldt, Substrate Channel in Nitrogenase Revealed by a Molecular Dynamics Approach, *Biochemistry*, 2014, **53**, 2278–2285, DOI: 10.1021/bi401313j.

86 I. Dance, Calculating the chemical mechanism of nitrogenase: new working hypotheses, *Dalton Trans.*, 2022, **51**, 12717–12728, DOI: 10.1039/d2dt01920e.

87 D. F. Harris, A. Badalyan and L. C. Seefeldt, Mechanistic Insights into Nitrogenase FeMo-Cofactor Catalysis through a Steady-State Kinetic Model, *Biochemistry*, 2022, **61**, 2131–2137, DOI: 10.1021/acs.biochem.2c00415.

88 L. Cao, O. Caldararu and U. Ryde, Protonation and Reduction of the FeMo Cluster in Nitrogenase Studied by Quantum Mechanics/Molecular Mechanics (QM/MM) Calculations, *J. Chem. Theory Comput.*, 2018, **14**, 6653–6678, DOI: 10.1021/acs.jctc.8b00778.

89 I. Dance, A molecular pathway for the egress of ammonia produced by nitrogenase, *Sci. Rep.*, 2013, **3**, 3237, DOI: 10.1038/srep03237.

90 I. Dance, The controlled relay of multiple protons required at the active site of nitrogenase, *Dalton Trans.*, 2012, **41**, 7647–7659, DOI: 10.1039/C2DT30518F.